Assessing rCBF Changes in Parkinson's Disease Using Independent Component Analysis

Jung-Lung Hsu[1], Jeng-Ren Duann[2,3], Han-Cheng Wang[1], Tzyy-Ping Jung[2,3]

[1]Department of Neurology, Shin Kong WHS Memorial Hospital, Taipei, Taiwan, ROC
[2]Computational Neurobiology Lab, the Salk Institute, La Jolla, CA 92037-5800, USA
[3]Institute for Neural Computation, University of California, San Diego, CA 92093 [jung@salk.edu]

ABSTRACT

Despite extensive studies in Parkinson's disease (PD) in recent decades, the neural mechanisms of this common neurodegenerative disease remain incompletely understood. Functional brain imaging technique such as single photon emission computerized tomography has emerged as a tool to help us understand the disease pathophysiology by assessing regional cerebral blood flow (rCBF) changes. This study applies Independent Component Analysis (ICA) to assess the difference in rCBF between PD patients and healthy controls to identify brain regions involving in PD. The brain areas identified by ICA include many regions in the basal ganglia, the brainstem, the cerebellum, and the cerebral cortex. Some of the regions have been largely overlooked in neuroimaging studies using region-of-interest approaches, yet they are consistent with previous pathophysiological reports. ICA thus might be valuable to suggest a new alternative disease and brain circuitry model in PD with a broader and more comprehensive aspect.

1. INTRODUCTION

Parkinson's disease (PD) is a common neurodegenerative disease that usually involves four cardinal motor features: resting tremor, bradykinesia, cogwheel rigidity and postural instability [1]. The pathophysiological mechanisms of PD remain largely unknown, but the primary neurotransmitter deficit appears mainly from the loss of dopaminergic (DA) nigrostriatal neurons in substantia nigra pars compacta [2], which results in loss of dopamine, mostly prominent in the striatum. According to the basal ganglia circuitry model [3,4], the loss of dopamine results in the abnormal activity in internal globus pallidus (GPi) both directly and indirectly, contributing to the movement abnormalities in PD. A common expectation is that this alteration of functional activity in basal ganglia might be consistently associated with changes in regional cerebral metabolism (rCMR) and regional cerebral blood flow (rCBF), although the correlation between the cardinal feature and cerebral substrate has not yet completely understood. Using ^{18}Ffluoro-2-deoxyglucose (FDG) positron emission tomography (PET), Lozza et al. [5] recently reported that bradykinesia scores were significantly positively correlated with rCMR in the bilateral putamen and globus pallidus, while tremor scores were negatively correlated with bilateral putamen and cerebellar vermis cerebral metabolic rate of glucose.

99mTc hexaemethyl-propyleneamine oxime (HMPAO) single photon emission computerized tomography (SPECT) is a well-established method to assess the rCBF that is also expected to co-vary with the disease progression in PD. However, previous results in SPECT have been mixed. The basal ganglia rCBF, for example, has been reported to be either reduced, increased or unchanged [7-9] in PD. Recently, Imon et al. [11] showed that adjusted rCBF increased in the bilateral putamen and the right hippocampus in patients with stage I or II PD, while adjusted rCBF increased bilaterally in the putamen, the globus pallidus, the hippocampus, the cerebellar hemispheres (dentate nuclei), the left ventrolateral thalamus, the right insula, and the right inferior temporal gyrus in patients with stage III or IV PD. Although the published literatures have not yet reached consensus on the brain areas co-varying with increasing severity of PD, one would expect that the increased rCBF should be found in the bilateral putamen, the bilateral globus pallidus, and the thalamus in the SPECT measurements. We also expect to find decreased rCBF in PD patients in brain areas involving in motor planning such as the premotor cortex (PM), the supplementary motor area (SMA) and the cerebellar cortices.

This study assesses the difference in rCBF between the forty-eight (48) healthy controls and twenty (20) PD using a data-driven statistic method, Independent component analysis (ICA). ICA decomposes the normalized SPECT dataset into components with maximally independent and spatially fixed regions whose rCBF change systematically from subject to subject or from subject group to subject group.

2. METHOD

Subjects

Twenty PD patients and forty eight normal-control volunteers participated in this study. Patients were diagnosed with PD according to the research diagnostic criteria suggested by Ward and Gibb [12] and staged based on the method of Hoehn and Yahr [13]. The 20 PD patients (17 male, 3 female; mean age of 66.1+ 10 years) were divided into two groups; 7 patients with Hoehn-Yahr stage I and 13 patients with stage III. The patients received anti-parkinsonian therapy with various combinations of L-DOPA with decarboxylase inhibitor (carbidopa), anticholinergic agents, amantadine hydrochloride and dopamine receptor agonist. Patients were imaged after at least one month of stable anti-parkinsonian therapy with optimal clinical benefit.

Forty-eight control subjects (16 male, 32 female; mean

age of 55.6 ± 10 years) were normal healthy volunteers who had no neurologic or psychiatric disorder, including alcoholism, substance abuse, head trauma with consciousness loss and cerebral vascular disorder. All subjects were given information about the procedure and all signed informed consents.

Experimental Protocol

Patients and control subjects were injected with 740MBq (20 mCi) of [99mTc] HMPAO 30 minutes prior to scanning. Scanning was performed parallel to the canthomeatal line using the dual-head Gamma Camera VariCam (GE, USA) with high resolution collimator (full width half maximum: 8 mm). A polycarbonate head holder was used to reduce head movement during scanning. The acquisition parameters were 120 projections recorded in step-and-shoot mode over a 360^o rotation arch (each head acquired 60 projections). The angular step was 3^o, and the frame time was 25 seconds per step. Each acquisition was completed in 30 minutes. The acquisition matrix was 128x128; zoom 1.5. All projection data were prefiltered with a Metz filter (cutoff at 54) which resulted in axial images at 128x128x80-pixel slices (1.77x1.77x1.8mm in actual size of voxel). Attenuation correction based on Chang's method [14] was performed for each slice, with a uniform attenuation coefficient 0.11.

Image Transformation

All images were first converted to Analyze format from their native image format using MRIcro software developed by Chris Rorden [http://www.psychology.nottingham.ac.uk/staff/crl/mricro.html]. For each subject, the brain images were re-oriented and spatially normalized to the standard MNI (Montreal National Institute) template included in SPM99 (http://www.fil.ion.ucl.ac.uk/spm/). The object brain masking was first created from the subject's images, co-registered with the default brain mask of SPM99 using the 12-parameter affine transformation. Then, non-linear algorithms with basis functions of 7x8x7, 12 non-linear iterations and medium nonlinear regularization were used to spatially normalize the subject's images to the SPM SPECT template. As a result, each subject's images were re-sampled into 2x2x2 mm along the directions of right-left, anterior-posterior, and superior-inferior, respectively.

Independent Component for Neuroimaging Data

First application of ICA to neuroimaging data was proposed by McKeown et al. [15,16] who demonstrated the usefulness of blind source separation for dissecting many types of activity from functional magnetic resonance imaging (fMRI) data of blood oxygen level-dependent (BOLD) contrast based on an information-maximization algorithm of Bell and Sejnowski [17]. In the studies, ICA derives spatially maximally independent components, though their time courses, the columns of inverse of unmixing matrix, may be correlated. Subsequent work has explored the applications of temporal ICA to fMRI data [18], in which ICA components were assumed to be temporally independent but spatially overlapped. Effort has also been made to use ICA for drawing group inferences from the fMRI [19]. However, all aforementioned studies applied ICA to spatio-temporal neuroimaging data. In this study, SPECT data do not contain any temporal information; instead they comprise 3-D neuroimaging data from multiple individuals. Therefore, it is important to note what are the assumptions underlying this application.

What are independent components of SPECT data?

For SPECT data analysis, the rows of the input matrix, **X**, are SPECT data from multiple individuals and the columns are measurements recorded at different voxels. ICA finds an `unmixing' matrix, **W**, that decomposes or linearly unmixes the SPECT data into a sum of spatially independent components, $\mathbf{C} = \mathbf{WX}$, where again, **X** is the $\boldsymbol{n}$ by $\boldsymbol{v}$ row mean-zero data matrix with $\boldsymbol{n}$ the number of subjects in the study and $\boldsymbol{v}$ the total number of voxels. **W** is an $\boldsymbol{n}$ by $\boldsymbol{n}$ unmixing matrix, and **C** is an $\boldsymbol{n}$ by $\boldsymbol{v}$ matrix of $\boldsymbol{n}$ spatially spatially-fixed three-dimensional independent "component maps" (sICs). If **W** is invertible, we can write, $\mathbf{X} = \mathbf{W}^{-1}\mathbf{C}$. The columns of $\mathbf{W}^{-1}$ represent signal strength of the brain voxels (defined by the component maps) used to construct the observed SPECT data, **X**. That is, the signal amplitudes in the columns of $\mathbf{W}^{-1}$ represent the relative rCBF strength of the brain regions recruited by the corresponding component map across subjects. We expect that some of the resultant components may account for the differences of rCBF changes between (normal vs PD) groups, while other components may account for subject variability in anatomy or rCBF. In this study, normalizing each subject's SPECT to the standard brain prior to analysis thus is very crucial because ICA will be overwhelmed by subject variability if normalization was not done properly. After the ICA training converged, we applied a simple statistic analysis (*t*-test) to the columns of $\mathbf{W}^{-1}$ to find components of interest and to test the significance of the rCBF difference between normal and patient groups. The components selected from the result of *t*-test between groups ($p<0.005$) delineate brain areas involving in PD.

3. RESULTS

Figure 1 shows three of the nine ICA components accounting primarily for the rCBF difference between subject groups in the SPECT data collected from 48 normal volunteers, 7 patients with Stage I PD and 13 patients with Stage III PD. In the 2D displays of Fig. 1, the warm colors (yellow and red) indicate the increased rCBF in PD, compared with normal (PD > normal); the cold colors (blue) indicate the decreased rCBF. In these figures, the brain areas showing increased rCBF in PD include the bilateral putamen, the globus pallidus, and sub-regions of the thalamus. For each ICA component map, we applied Talairach Daemon, a freely available software on the Internet, to convert the coordinates of brain areas to the anatomical naming.

Table 1 lists the brain areas with significant rCBF changes between groups (PD1 + PD3 > normal and vice

(A)

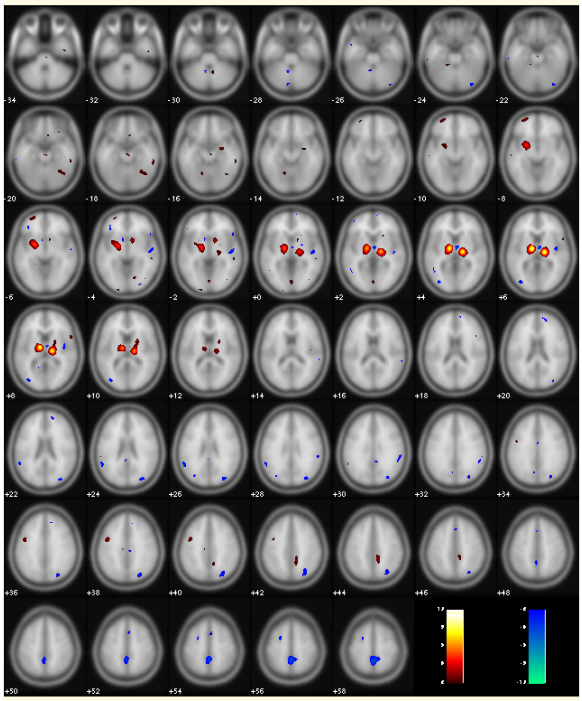

(B)

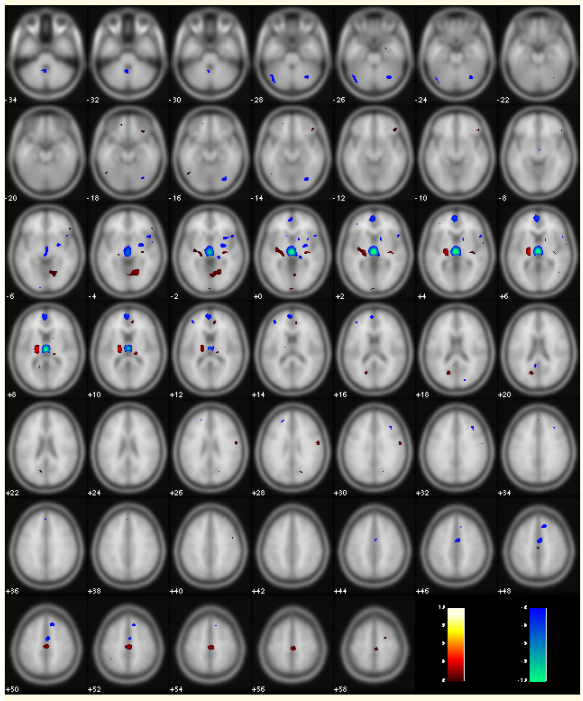

(C)

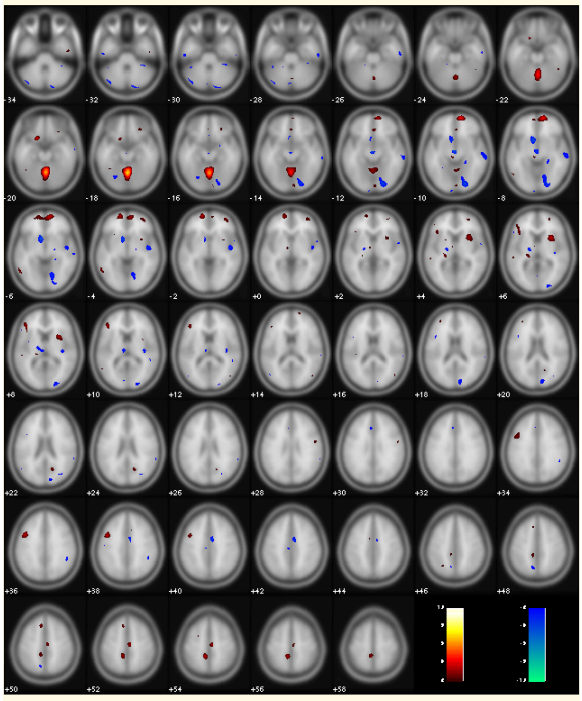

(D)

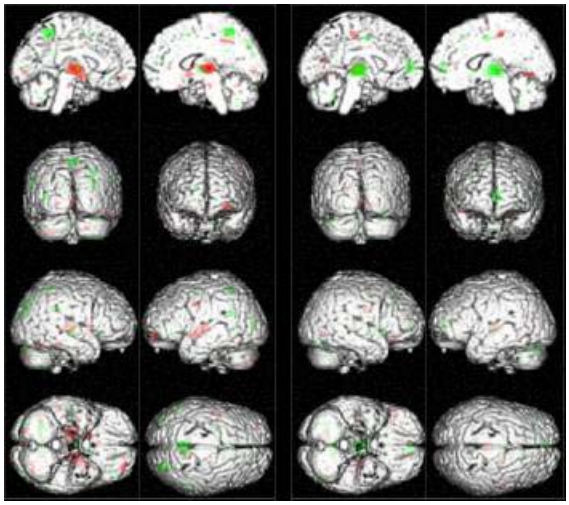

Fig. 1 Highlighted brain areas show significant rCBF changes in Parkinson's disease, compared with normal controls.(A), (B) and (C) Component maps of three of nine ICA components accounting for rCBF changes between subject groups. The warm colors (e.g. yellow, red) indicate the brain areas with rCBF changes of (PD1 + PD3) > Normal, and the cold colors (e.g. blue) show opposite changes (with *t*-test, $p < 0.005$). (d) The same results in (A) and (B) were plotted on a 3-D rendered brain template from SPM'99.

versa, both with $p < 0.005$). Only voxels (brain areas) with z-values greater than 4 ($z > 4$) were listed in Table 1 [20]. Under the column of PD > normal, the bilateral putamen, the globus pallidus, some sub-regions of the thalamus and the pons were identified, which were the target brain areas according to the previous literatures. In addition, we found increased rCBF in the bilateral amygdala, the right middle frontal gyrus, the left hippocampus, the left subcollosal gyrus, the bilateral anterior cerebellum and the midbrain. Contrast to the finding of Lozza et al. [5], the cerebellar vermis showed increased rCBF in PD.

Under the column of normal > PD, the decreased rCBF was found in the bilateral insula, the bilateral cingulated gyrus, the paracentral lobule, the precuneus, the left supramarginal gyrus, the left superior temporal gyrus, the right cuneus, the bilateral cerebellar culmen and the declive. Details please see Table 1.

4. DISCUSSION

Measurements of rCBF with SPECT have been used as an effective method to study the functional organization of the human cortex for decades. HMPAO is a reliable indicator of cerebral blood flow [21,22] and can approximate perfusion images derived from xenon-133 measurement [23]. However, comparisons of rCBF between PD and control remain very controversial and heterogeneous in previous studies. In this study, we applied ICA to voxel-base images to systemically and objectively assess rCBF changes between groups. Our results showed that many brain areas having significant rCBF differences between groups are consistent with the previously neuropathological studies and the prediction of the basal ganglia circuitry model.

rCBF increased in PD

In this study, we found rCBF increased in PD in the basal ganglia area, the cerebral cortex, the brainstem and the cerebellum. Within these areas, increased rCBF in the bilateral putamen, the globules pallidum, the thalamus, and the pons are expected by the basal ganglia circuit model [3,4] and consistent with the previous studies in SPECT and FDG-PET. Based on scaled subprofile model (SSM), a method based on principle analysis of region-of-interest (ROI), Eidelberg et al [24] reported a metabolic topographic profile of PD, "Parkinson's disease-related profile", which comprises a relative hypermetabolism of the lentiform nucleus, the thalamus and the pons, and a relative hypometabolism of the lateral frontal cortex. Bradykinesia, a major key motor feature in PD, also showed a positive correlation with putamen glucose metabolism by a FDG-PET study in resting state [5]. The reason of increased rCBF in the amygdala and the hippocampus however remains unclear. Increased rCBF in these regions had also been reported by Imon et al[12]. The basal ganglia has been reported to participate in the limbic process [4], which might contribute to neuropsychiatric manifestations in PD. Group rCBF difference in the cerebellum has also been found in the present study. SPECT and FDG-PET studies in this area, however, have been contradictory. Our results showed mosaic patterns in the cerebellar vermis and hemisphere such as dentate nucleus. The increased rCBF found in our study in the dentate nucleus is consistent with a previous report by Imon et al [12]. In Lozza's study [5], tremor was negatively correlated with cerebellar vermis. However, in a PET study using FDG and F-dopa, Ghaemi et al. [25] demonstrated that monosymptomatic resting tremor represented a phenotype of PD, with a nearly identical striatal dopaminergic deficit and postsynaptic D2-receptor upregulation in PD's patients. They further suggested that the cerebellar metabolic hyperactivity in PD was closely related to akinesia and rigidity rather than to tremor.

rCBF decreased in PD

Decreased rCBF in PD was found mostly in the cerebral cortex. In additions, the caudate, the medial dorsal nucleus of the thalamus, the midbrain and the cerebellum also showed decreased rCBF in PD. The involved cortices included the cingulate, the insula, the lateral temporal lobe, the inferior parietal lobe and the precuneus. Decreased rCBF in temporo-parietal cortex might be due to two reasons: autonomic failure or cognitive impairment. Arahata et al. [26] reported that rCMR in the cerebral cortex in PD with autonomic failure was markedly reduced, compared with normal, particularly in the occipital cortex, the inferior parietal cortex, and the superior parietal cortex, but no decrease in the sensory motor and the medial temporal cortices, the putamen and the thalamus. Their findings raised the possibility that PD with autonomic failure may overlap with the features of dementia with Lewy bodies. Antonini et al [27] exploited the SPECT to study PD with cognitive impairment and found that, compared with healthy controls, demented PD patients showed significant perfusion decrements in all the cortical areas, particularly in the temporal and the parietal regions. However, in the non-demented PD, reductions in rCBF were limited to the frontal lobe area. On the contrary, Hu et al. [28] applied partial volume effect correction to posterior parietal and temporal regions of (31)P magnetic resonance spectroscopy (MRS) and FDG-PET and found statistically significant hypometabolism in the temporoparietal cortex for non-demented PD patients compared with controls, suggesting that both glycolytic and oxidative pathways were impaired. This dysfunction may reflect either the presence of primary cortical pathology or deafferentation of striato-cortical projections. They also suggested that hypometabolism in the temporoparietal cortex could be a useful predictor of future cognitive impairment in the non-demented PD. Decreased rCBF in the precuneus was also noted in the early stage of Alzheimer's disease [29]. Either autonomic failure or cognitive impairment suggests the patient with PD may combine with other underlying neuropathological changes such as Lewy body pathology in our patients. Hypoperfusion of the insula and the cingulate cortices were also noted in the present study, consistent with the extended prediction of the basal ganglia circuitry model. Mixed rCBF results (increased [12] or decreased [30]) in the insula have been reported in the past.

Kikuchi et al [31] used the HMPAO-SPECT and SPM method to study the PD patients and reported decreased rCBF in the SMA, the dorsolateral prefrontal cortex and the insular cortex in PD. In the cingulate gyrus, most of the PET and SPECT studies did not find any decrease in rCMR or rCBF. However, in a SPECT study on PD treated with deep-brain stimulation of subthalamic nucleus (STN), Sestini et al [32] reported significant rCBF increase in the right pre-supplementary motor area (pre-SMA), the anterior cingulate cortex, the dorsolateral prefrontal cortex and the medial Brodmann's area 8 when the deep-brain stimulation was ON, and the rCBF decreased when the deep-brain stimulation was OFF. Their results provided the direct evidence of the association between the basal ganglia circuitry and the limbic system, which may involve in the higher-order aspects of motor control.

rCBF Changes in Substantia nigra

It is worth mentioning that we also found decreased rCBF in the substantia nigra in PD patients, compared with normal controls. This region, however, is not listed in Table 1 because the z-value (z=2.71) of the voxels in the area does not exceed our strict threshold (z>4). The sub-threshold value may be partially due to the limitations of attenuation correction of SPECT in brain deep structure. According to basal ganglia circuitry model, the neuronal loss in this region is the cause of clinical motor features of PD. It is thus reasonable to expect that rCBF or rCMR will decrease in this area. However, until now, only the neuropathological study has demonstrated the neuronal loss in this region [33]. Even the nuclear medicine image used in the ligand of dopaminergic system [34,35], has only demonstrated the loss of dopaminergic activity in the striatum, which remains an indirect evidence of dopaminergic neuronal loss in the substantia nigra area. Our result may be the first direct evidence to the well-anticipated decreased rCBF in this pathogenic region in PD. We are currently investigating the accuracy and replicability of this result in a larger subject pool.

Table 1 List of brain areas having significant rCBF changes between the PD patients and controls.

Brain areas	**(PD1 + PD3) > Normal**	**Normal > (PD1 + PD3)**
Cerebral cortex	Bilateral Precentral Gyrus Bilateral Postcentral Gyrus Bilateral Amygdala Right Middle Frontal Gyrus Left Hippocampus Left Subcollosal Gyrus (BA 34)	Bilateral Cingulate (BA 31) Bilateral Insula Bilateral Paracentral Lobules (BA 5) Bilateral Precuneus (BA 7, 31) Right Cuneus Left Superior Temporal Gyrus Left Supramarginal Gyrus Left Lingual Gyrus
Basal ganglion	Bilateral Lentiform Nucleus Medial Globus Pallidus Lateral Globus Pallidus Putamen Bilateral Thalamus Ventral Posterior Medial Nucleus Ventral Posterior Lateral Nucleus Mammilary Body, Pulvinar	Bilateral Thalamus Medial Dorsal Nucleus Left Caudate
Brain stem	Bilateral Brainstem Medula, Pons	Bilateral Midbrain Red Nucleus
Cerebellum	Bilateral Cerebellum Culmen, Fastiguim Dentate Nucleus, Nodule Tonsil, Declive Declive of Vermis, Pyramis	Bilateral Cerebellum Tuber, Uvula, Declive, Declive of Vermis, Pyramis

5. CONCLUSIONS

In this present study, we assess the rCBF changes between PD patients and normal controls using Independent Component Analysis. The brain areas showing increased and decreased rCBF are consistent with previous pathophysiological reports in PD. The most prominent finding in this report is that ICA finds many significant rCBF changes in the cerebral cortex, which has been largely overlooked by the previous studies using region-of-interest approaches. Furthermore, the cortical involvement in our findings is more prominent than the study of Imon et al [12] using SPM approach. Our results did not show significant group rCBF changes in the SMA or the PM, which were thought to be involved in the motor planning in PD. This might be in part due to the fact that our subjects were on medication and scanning was done during resting.

The use of ICA can complement hypothesis-driven methods for analyzing SPECT data because: (1) ICA does not rely on *a priori* knowledge of the involvement of brain regions in PD. (2) ICA can be used to separate the component processes accounting for disease-related metabolic responses, non-disease related physiological phenomena and subject anatomical variability. ICA thus

might be able to reveal additional connections, interactions or associations between different brain areas in PD, which might have been overlooked by some hypothesis-driven methods. Furthermore, this ICA-based data-driven approach may help or suggest neurologists to consider alternative disease and brain circuitry model in PD or other neurodegenerative diseases with a broader and more comprehensive aspect.

REFERENCES

[1] Parkinson J. (1817). An essay on the shaking palsy. London: printed by Whittingham and Rowland for Sherwood, Neely and Jones.

[2] Hornykiewcz O. (1966), Dopamine (3-hydroxytyramine) and brain function. *Pharmacol Rev.* 18:925-964.

[3] Albin RL, Young AB, Penney JB. (1989), The functional anatomy of basal ganglia disorders. *Trends Neurosci* 12:366-75.

[4] Alexander GE, Crutcher MD. (1990), Functional architecture of basal ganglia circuits: neural substrates of parallel processing. *Trends Neurosci* 13:266-71.

[5] Lozza C, Marie RM, Baron JC. (2002), The metabolic substrates of bradykinesia and tremor in uncomplicated Parkinson's disease. *Neuroimage* 17:688-99.

[6] Henriksen L, Boas J. (1985), Regional cerebral blood flow in hemiparkinsonian patients: emission computerized tompgraphy of inhaled 133Xenon before and after levodopar. *Acta Neurol Scand*. 1985;71:257-266.

[7] Perlmutter JS, Raichle ME. (1985): Regional blood flow in hemiparkinsonism. *Neurology* 35:1127-34.

[8] Wolfson LI, Leenders KL, Brown LL, Jones T. (1985). Alterations of cerebral blood flow and oxygen metabolism in Parkinson's disease. *Neurology* 35:1399-1405.

[9] Pizzolato G, Dam M, Borsato N, et al. (1888), [99mTc]-HMPAO SPECT in Parkinson's disease. *J Cereb Blood Flow Metab.* 8(suppl):S101-S108.

[10] Wolfson LI, Leenders KL, Brown LL, Jones T. (1985), Alterations of regional cerebral flow and oxygen metabolism in Parkinson's disease. *Neurology* 25:1399-1405.

[11] Imon Y, Matsuda H, Ogawa M, Kogure D, Sunohara N. (1999), SPECT image analysis using statistical parametric mapping in patients with Parkinson's disease. *J Nucl Med.* 40;1583-89.

[12] Ward CD, Gibb WR. (1990), Research Diagnostic Criteria for Parkinson's disease. In Streifler M, Korczyn AD, Melamed E, Youdim MBH (eds). *Advances in Neurology* (53),245-249.

[13] Hoehn MM, Yahr MD.(1967), Parkinsonism: onset, progression and mortality. *Neurology*. 17:427-42.

[14] Chang LT. (1978), A method for attenuation correction in radionuclide computed tomography. *IEEE Trans Nucl Sci.* NS-25:638-43.

[15] McKeown M, Jung T-P., Makeig S, Brown GG, Kindermann S, Lee and Sejnowski TJ (1998) Spatially Independent Activity Patterns in Functional Magnetic Resonance Imaging Data During the Stroop Color-naming Task, *Proc. of the Natl Acad of Sci,* 95:803-10.

[16] McKeown M, Makeig S, Brown GG, Jung T-P, Kindermann S, Bell AJ and Sejnowski TJ (1998) Analysis of fMRI data by blind separation into independent spatial components, *Human Brain Mapping*, 6:160-88.

[17] Bell AJ and Sejnowski TJ (1995) An information maximization approach to blind separation and blind deconvolution. *Neural Comput.* 7, 1129–1159.

[18] Biswal BB, Ulmer JL (1999) Blind source separation of multiple signal sources of fMRI data sets using independent component analysis. *J Comput Assist Tomogr* 23:265–271.

[19] Calhoun VD, Adali T, Pearlson GD, Pekar JJ. (2001) A method for making group inferences from functional MRI data using independent component analysis, *Human Brain Mapping*, 14(3):140-51.

[20] Duann J-R, Jung T-P, Kuo W-J, Yeh T-C, Makeig S, Hsieh J-C, and Sejnowski TJ, (2002) Single-trial variability in event-related BOLD signals, *Neuroimage* 15, 823-835.

[21] Neirinckx RD, Canning LR, Piper IM Nowotnik DP, Pickett RD, Holmes RA, Volkert WA, Forster AM et al. (1987), Technetium-99m d.l-HM-PAO: a new radiopharmaceutical for SPECT imaging of regional cerebral blood perfusion. *J Nucl Med* 28(2): 191-202.

[22] Podreka I, Suess E, Goldenberg G, Steiner M, Brucke T, Muller C, Lang W, Neirinckx RD, Deecke L. (1987), Initial experience with technetium-99m HMPAO brain SPECT. *J Nucl Med* 28(11):1657-66.

[23] Payne JK, Trivedi MH, Devous MD Sr. (1996), Comparison of technetium-99mHMPAO and xenon-133 measurements of regional cerebral blood flow by SPECT. *J Nucl Med* 37(10): 1735-40.

[24] Eidelberg D., Moeller, J.R., Dhawan V., Septsieris, P., Takikawa., S., Ishikawa, T., Chaly, T., Robeson, W., Margouleff, D., and Przedborski, S. (1994). The metabolic topography of Parkinsonism. *J Cereb. Blood flow Meta.* 14:783-801.

[25] Ghaemi M, Raethjen J, Hilker R, Rudolf J, Sobesky J, Deuschl G, Heiss WD. (2002), Monosymptomatic resting tremor and Parkinson's disease: A multitracer positron emission tomographic study. *Mov Disord* Jul;17(4):782-8.

[26] Arahata Y, Hirayama M, Ieda T, Koike Y, Kato T, Tadokoro M, Ikeda M, Ito K, Sobue G. (1999), Parieto-occipital glucose hypometabolism in Parkinson's disease with autonomic failure. *J Neurol Sci.*163(2):119-26.

[27] Antonini A, De Notaris R, Benti R, De Gaspari D, Pezzoli G. (2001), Perfusion ECD/SPECT in the characterization of cognitive deficits in Parkinson's disease. *Neurol Sci.* 22(1):45-6.

[28] Hu MT, Taylor-Robinson SD, Chaudhuri KR, Bell JD, Labbe C, Cunningham VJ, Koepp MJ, Hammers A, Morris RG, Turjanski N, Brooks DJ. (2000), Cortical dysfunction in non-demented Parkinson's disease patients: a combined (31)P-MRS and (18)FDG-PET study. *Brain* 123(Pt 2):340-52.

[29] Matsuda H, (2001). Cerebral blood flow and metabolic abnormalities in Alzheimer's disease. A*nn Nucl Med* . 15(2):85-92.

[30] Kikuchi A, Takeda A, Kimpara T, Nakagawa M, Kawashima R, Sugiura M, Kinomura S, Fukuda H, Chida K, Okita N, Takase S, Itoyama Y. (2001), Hypoperfusion in the supplementary motor area, dorsolateral prefrontal cortex and insular cortex in Parkinson's disease. *J Neurol Sci* 193(1):29-36.

[31] Kikuchi A, Takeda A, Kimpara T, Nakagawa M, Kawashima R, Sugiura M, Kinomura S, Fukuda H, Chida K, Okita N, Takase S, Itoyama Y. (2001), Hypoperfusion in the supplementary motor area, dorsolateral prefrontal cortex and insular cortex in Parkinson's disease. *J Neurol Sci.* Dec 15;193(1):29-36.

[32] Sestini S, Scotto di Luzio A, Ammannati F, De Cristofaro MT, Passeri A, Martini S, Pupi A. 2002, Changes in regional cerebral blood flow caused by deep-brain stimulation of the subthalamic nucleus in Parkinson's disease. *J Nucl Med*, Jun;43(6):725-32.

[33] Fearnley JM, Lees AJ. (1991), Aging and Parkinson's disease: substantia nigra regional selectivity. *Brain* 114:2283-2301.

[34] Nahmias C, Garnett ES, Firnau G, Lang A. (1985), Striatal dopamine distribution in Parkinsonian patients during life. *J Neurol Sci* 69:223-230.

[35] Bao SY, Wu JC, Luo WF, Fang P, Liu ZL, Tang J, (2000). Imaging of dopamine transporters with technetium-99m TRODAT-1 and single photon emission computed tomography. *J Neuroimaging,* 10(4):200-3.